

Self-consistent mixed-basis approach to the electronic structure of solids

Steven G. Louie

IBM Thomas J. Watson Research Center, Yorktown Heights, New York 10598
and Department of Physics, University of California, Berkeley, California 94720*

Kai-Ming Ho and Marvin L. Cohen

*Department of Physics, University of California, Berkeley, California 94720
and Molecular and Materials Research Division, Lawrence Berkeley Laboratory, Berkeley, California 94720*

(Received 28 August 1978)

A mixed-basis method is developed for the calculation of the electronic structure of solids. The method is shown to be capable of treating crystals with large complex unit cells. A combined set of plane waves and Bloch sums of localized functions is employed as basis functions, thus leading to a very efficient representation of systems which contain both highly localized (atomiclike) and delocalized (plane-wave-like) electrons. The crystalline potential is determined in a fully self-consistent manner with no approximations made to its shape. The present method has the flexibility of being easily applicable to the study of many different systems (e.g., surface calculations with supercells). Specific application is made to bulk Nb and Pd to demonstrate the efficiency and accuracy of the method. Very good agreement with experimental results and with band structures calculated using other methods is obtained. It is found that, with a mixed basis, only a relatively small set of functions is needed to obtain convergent wave functions for the electrons.

I. INTRODUCTION

There has been a great deal of interest in the electronic structure of systems involving transition-metal atoms in recent years. The reasons vary according to the systems: transition-metal surfaces¹ (Ni, Pd, Pt, . . .) because of their catalytic properties; *A-15* compounds² (Nb₃Ge, V₃Si, . . .) because of their unusually high superconducting transition temperatures and their unusual transport properties; and transition-metal silicides³ (Pd₂Si, WSi₂, . . .) because of their importance in Si technology. Since these systems are composed of transition-metal atoms situated in an open structure and/or with group-IV elements which tend to form covalent bonds, traditional approaches [e.g., augmented plane-wave (APW), tight-binding, and plane-wave pseudopotential methods] are found to be inconvenient when used to calculate the electronic properties of these systems. This situation motivated us to develop and utilize a mixed-basis approach for studying the electronic structure of the above-mentioned and other related systems.

The main features of the present method include the following: (i) An energy-independent basis set which contains both plane waves and localized functions is used for the expansion of the electronic wave functions. (ii) Infinite-range interactions between basis functions are retained. (iii) No shape approximations to the potential (such as that of muffin-tin form) are made. And (iv) the calculations are carried out in a self-con-

sistent-field fashion with the effects of exchange and correlation included via a local-density theory.^{4,5}

The present approach has a number of advantages over traditional methods. Because the basis functions employed combine the important physical aspects of a set of plane waves with those of a set of Bloch sums of localized functions, this approach is especially suitable for systems characterized by electronic wave functions which contain both highly localized (atomic like) and delocalized (plane-wave-like) components. Tight-binding methods have difficulties in treating the electron wave function and potential in the interstitial regions in a convenient and unbiased way.⁶ Plane-wave methods have difficulties in reproducing the atomic character of the *d* wave function near the atomic core. Also since, unlike standard APW or Korringa-Kohn-Rostoker (KKR) methods, muffin-tin or other shape approximations to the potential have not been made, electrons in systems with open structure or those at surfaces and interfaces can be treated straightforwardly and accurately using this method. Finally, the present method goes beyond previous mixed-basis attempts⁷⁻¹² in that the Hamiltonian matrix elements are evaluated accurately in a first-principles fashion and, more importantly, the calculations are carried out self-consistently within the pseudopotential formalism. The calculations are therefore parameter free and the method has the flexibility of being easily applicable to the study of many different systems.

In this paper we describe the formulation of the

method in some detail. As examples, the method has been used to calculate the electronic structure of bulk Nb and Pd representing the two extremes of the 4d transition-metal series. The results obtained are in very good agreement with experiments and with results calculated using other methods. It is found that only a relatively small set of basis functions per atom¹³ is needed to obtain convergent wave functions for the electrons. This aspect of the method has the important consequence of making self-consistent calculations possible for systems which have large numbers of atoms per unit cell (e.g., surface calculations involving supercells¹⁴ or the A-15 compounds¹⁵).

The remainder of the paper is organized as follows: In Sec. II the mixed-basis pseudopotential method is discussed. The important concepts and various working equations in the formalism are derived. In Sec. III the results for the electronic structure of Nb and Pd are presented and the accuracy and efficiency of the method is evaluated. Finally, in Sec. IV a summary and some discussions are presented.

II. MIXED-BASIS PSEUDOPOTENTIAL FORMALISM

A. The Hamiltonian

The starting point of all electronic-structure calculations is the construction of the effective one-electron Hamiltonian. In the self-consistent-pseudopotential approach, the pseudo-Hamiltonian for the valence and the conduction-band states has the general form

$$H = p^2/2m + V_{ps} + V_H + V_{xc}, \quad (1)$$

where

$$V_{ps} = \sum_{\vec{R}_n, \vec{\tau}_a} V_a^{ion}(\vec{r} - \vec{R}_n - \vec{\tau}_a) \quad (2)$$

is a superposition of bare ionic pseudopotentials (e.g., in the case of Pd, V_{Pd}^{ion} is the ionic pseudopotential appropriate to the Pd¹⁰⁺ ion). The ionic pseudopotential is screened by a Hartree potential V_H and a local exchange-correlation potential V_{xc} obtained from the pseudo-valence-charge density ρ by

$$\nabla^2 V_H(\vec{r}) = -4\pi e^2 \rho(\vec{r}) \quad (3)$$

and

$$V_{xc} = -3e^2(3/8\pi)^{1/3} \alpha \rho(\vec{r})^{1/3}, \quad (4)$$

where α is a function of¹⁶ $\rho(\vec{r})$ or simply chosen to be a constant (the $X\alpha$ method).¹⁷ The energies and wave functions of the electrons are obtained by iterating Eqs. (1), (3), and (4).¹⁸

The fundamental advantage of using pseudopo-

tentials¹⁹ is that the core states are eliminated from the problem. Unlike the real wave functions, the pseudo wave functions are relatively smooth. (They need not be orthogonal to the core-state wave functions.) One consequence of this is that the localized functions in the basis set are quite simple since they, together with the plane waves, are only required to reproduce the behavior of the pseudoatom near the atomic core. This feature therefore greatly simplifies the evaluation of V_H and V_{xc} and the various Hamiltonian matrix elements, making self-consistent calculations feasible.

In the pseudopotential approach, the ionic pseudopotential is, however, in general a non-local operator. For electrons with energies over a range of 20–30 eV about the Fermi level, the ionic pseudopotential for transition metals is an l -dependent potential of the form

$$V^{ion} = V_0(|\vec{r}|) + \sum_{l=1}^2 \delta V_l(|\vec{r}|) P_l, \quad (5)$$

where P_l is the projection operator acting on the l th angular-momentum component of the wave function. V_0 , δV_1 , and δV_2 are determined by fitting to the energies and wave functions of an all-electron calculation of the neutral atom in various atomic configurations using the same exchange-correlation functional.

B. Basis set and evaluation of matrix elements

In the mixed-basis approach, as in most band-theoretical methods, the electronic wave function is expanded in a set of basis functions and the solutions to the Schrödinger equation are obtained by variational procedures. Since the computational effort increases at least as fast as the third power of the number of basis functions used, it is of utmost importance, for computational purposes, to choose a small, yet *physically* complete, set of functions. A judicious choice, as discussed in the Introduction, is a combined set of plane waves and localized functions.

For each \vec{k} in the Brillouin zone, the basis set consists of plane waves

$$\frac{1}{\sqrt{\Omega}} e^{i(\vec{k} + \vec{G}) \cdot \vec{r}} \quad (6)$$

and Bloch sums of local orbitals

$$\phi_{i\mu}(\vec{k}, \vec{r}) = \frac{1}{\sqrt{\Omega}} \sum_{\vec{R}} e^{i\vec{k} \cdot (\vec{R} + \vec{\tau}_i)} f_{i\mu}(\vec{r} - \vec{R} - \vec{\tau}_i), \quad (7)$$

where \vec{G} is a reciprocal-lattice vector, \vec{R} is a lattice vector, $\vec{\tau}_i$ is a basis vector, μ is a label for the orbitals on the i th atom, and Ω is the crystal volume. In the present formulation, the

localized functions $f_{i\mu}(\vec{r})$ can be either simple orbitals (such as Gaussian or Slater orbitals) or numerical functions. The electron wave function is expanded in

$$\psi_{\vec{k}}(\vec{r}) = \frac{1}{\sqrt{\Omega}} \sum_{\vec{G}} \alpha(\vec{k} + \vec{G}) e^{i(\vec{k} + \vec{G}) \cdot \vec{r}} + \sum_{i\mu} \beta_{i\mu}(\vec{k}) \phi_{i\mu}(\vec{k}, \vec{r}), \quad (8)$$

which leads to the following matrix eigenvalue problem

$$(H - ES)\Lambda = 0, \quad (9)$$

where H is the Hamiltonian matrix, S is the overlap matrix, and Λ is a column vector with elements $\lambda_1, \dots, \lambda_n$ corresponding to the expansion coefficients α, β in Eq. (8).

We find that the most convenient and accurate way of obtaining the matrix elements of H and S is to make use of the periodicity of the crystal and evaluate these quantities in reciprocal space.^{20,21} This procedure allows the inclusion of the effects of long-range overlaps between the basis functions without the complication of calculating multicenter integrals in real space. The ϕ 's are expanded in plane waves of reciprocal-lattice vectors,

$$|\phi_{i\mu}(\vec{k}, \vec{r})\rangle = \sum_{\vec{G}} T_i(\vec{G}) f_{i\mu}(\vec{k} + \vec{G}) |\vec{k} + \vec{G}\rangle, \quad (10)$$

where T_i which contains the structural information is

$$T_i(\vec{G}) = e^{-i\vec{G} \cdot \vec{r}_i} / M, \quad (11)$$

where M is the number of atoms per unit cell and $f_{i\mu}(\vec{k} + \vec{G})$ which is independent of the crystal structure is the Fourier transform of the localized functions,

$$f_{i\mu}(\vec{k} + \vec{G}) = \frac{1}{\Omega_a} \int e^{-i(\vec{k} + \vec{G}) \cdot \vec{r}} f_{i\mu}(\vec{r}) d^3r, \quad (12)$$

with Ω_a the atomic volume. The expansion in Eq. (10) usually involves many more plane waves than those in the basis set because of the localized

nature of $f_{i\mu}$. When $f_{i\mu}$ is chosen to be a Gaussian or Slater orbital, $f_{i\mu}(\vec{k})$ is a simple analytic function of \vec{k} . The three types of overlap matrix elements in this scheme are then simply

$$S_{\vec{k} + \vec{G}, \vec{k} + \vec{G}'} = \langle \vec{k} + \vec{G} | \vec{k} + \vec{G}' \rangle = \delta_{\vec{G}\vec{G}'}, \quad (13)$$

$$S_{\vec{k} + \vec{G}, i\mu} = \langle \vec{k} + \vec{G} | \phi_{i\mu}(\vec{k}, \vec{r}) \rangle = T_i(\vec{G}) f_{i\mu}(\vec{k} + \vec{G}), \quad (14)$$

and

$$S_{i\mu, j\nu} = \langle \phi_{i\mu}(\vec{k}, \vec{r}) | \phi_{j\nu}(\vec{k}, \vec{r}) \rangle \\ = \sum_{\vec{G}} T_i^*(\vec{G}) f_{i\mu}^*(\vec{k} + \vec{G}) T_j(\vec{G}) f_{j\nu}(\vec{k} + \vec{G}). \quad (15)$$

The evaluation of the Hamiltonian matrix elements is slightly more involved. To simplify the discussions to follow, we rewrite the Hamiltonian [Eq. (1)] in the form (in Ry units)

$$H = -\nabla^2 + V_L + V_{NL}, \quad (16)$$

where V_L is the local part of the ionic pseudopotential added to $V_H + V_{xc}$ and V_{NL} is the angular-momentum-dependent part of the ionic pseudopotential. The matrix elements of H between the plane waves are evaluated in the same way as in standard nonlocal pseudopotential calculations,¹⁹ i.e.,

$$\langle \vec{k} + \vec{G} | H | \vec{k} + \vec{G}' \rangle = |\vec{k} + \vec{G}|^2 \delta_{\vec{G}\vec{G}'} + V_L(\vec{G} - \vec{G}') \\ + V_{NL}(\vec{k} + \vec{G}, \vec{k} + \vec{G}'). \quad (17)$$

The cross terms are given by

$$\langle \vec{k} + \vec{G} | H | \phi_{i\mu}(\vec{k}, \vec{r}) \rangle = \sum_{\vec{G}'} [|\vec{k} + \vec{G}|^2 \delta_{\vec{G}\vec{G}'} + V_L(\vec{G} - \vec{G}')] \\ \times T_i(\vec{G}') f_{i\mu}(\vec{k} + \vec{G}') \\ + \sum_{\vec{G}'} V_{NL}(\vec{k} + \vec{G}, \vec{k} + \vec{G}') \\ \times T_i(\vec{G}') f_{i\mu}(\vec{k} + \vec{G}'). \quad (18)$$

And the terms between the Bloch sums of localized functions are given by

$$\langle \phi_{j\nu}(\vec{k}, \vec{r}) | H | \phi_{i\mu}(\vec{k}, \vec{r}) \rangle = \sum_{\vec{G}} |\vec{k} + \vec{G}|^2 T_j^*(\vec{G}) f_{j\nu}^*(\vec{k} + \vec{G}) T_i(\vec{G}) f_{i\mu}(\vec{k} + \vec{G}) \\ + \sum_{\vec{G}, \vec{G}'} T_j^*(\vec{G}) f_{j\nu}^*(\vec{k} + \vec{G}) V_L(\vec{G} - \vec{G}') T_i(\vec{G}') f_{i\mu}(\vec{k} + \vec{G}') \\ + \sum_{\vec{G}, \vec{G}'} T_j^*(\vec{G}) f_{j\nu}^*(\vec{k} + \vec{G}) V_{NL}(\vec{k} + \vec{G}, \vec{k} + \vec{G}') T_i(\vec{G}') f_{i\mu}(\vec{k} + \vec{G}'). \quad (19)$$

As seen from Eqs. (13)–(19), the matrix elements for both H and S can be calculated quite straightforwardly with the structural information contained solely in the $T_i(\vec{G})$'s and the structural factors in the Fourier coefficients of the ionic crystalline potential. The most time-consuming part of evaluating these matrix elements is the second and third term on the right-hand side of Eq. (19) which involves N^2 operations if N is the number of \vec{G} vectors needed to expand $\phi_{i\mu}(\vec{k}, \vec{r})$. However, both terms can be reformulated to reduce the computational effort by orders of magnitude. The second term, $\langle \phi_{j\nu} | V_L | \phi_{i\mu} \rangle$, may be evaluated by first transforming $\phi_{j\nu}^*(\vec{k} + \vec{G})$, $\phi_{i\mu}(\vec{k} + \vec{G})$ and $V_L(\vec{G})$ to real space using the fast-Fourier-transform approach (which involves $N \ln N$ operations) and then summing in real space (which involves N operations). This procedure thus reduces the number of operations from N^2 to $N \ln N$, a huge saving if N is large. Furthermore since δV_i is nonzero only in the ionic core region, V_{NL} is a sum of extremely short-range operators centered on each atomic site. Also, if N is large, the $\phi_{i\mu}$'s are then sums of short-range functions centered on each atomic site. This feature of V_{NL} and the ϕ 's allows the third term in Eq. (19), $\langle \phi_{j\nu} | V_{NL} | \phi_{i\mu} \rangle$, to be calculated (at least for the case of the d orbitals for transition-metal atoms) to a high degree of accuracy using an on-site approximation, i.e.,

$$\langle \phi_{j\nu} | V_{NL} | \phi_{i\mu} \rangle = \frac{1}{\Omega_a} \sum_{\vec{r}} \int f_{j\nu}^*(\vec{r}) \delta V_i(|\vec{r}|) \times P_i f_{i\mu}(\vec{r}) d^3r \delta_{ij}. \quad (20)$$

Note that the above expression involves only single-site integrals and it is independent of the \vec{k} point under consideration.

C. Self-consistent procedure

To obtain self-consistent solutions to the matrix eigenvalue problem, Eq. (9), we use the following procedure. Equation (9) is first transformed into the standard form

$$(H' - E)\Lambda' = 0, \quad (21)$$

where H' is also a Hermitian matrix. This can be achieved by using the Choleski scheme,²² i.e., by decomposing the overlap matrix S into a product of a lower triangular matrix and its Hermitian conjugate

$$S = LL^\dagger. \quad (22)$$

Then Eq. (9) is related to Eq. (21) by

$$H' = L^{-1}H(L^{-1})^\dagger \quad (23)$$

and

$$\psi = (L^{-1})^\dagger \psi'. \quad (24)$$

The matrix elements of L^{-1} can be easily obtained from the matrix elements of S in a straightforward, iterative fashion. (See Appendix A.) If we have solved the problem for an $n \times n$ matrix of S , then for this matrix extended to the size $(n+1) \times (n+1)$ the additional elements of L^{-1} are given by the following recursion relations

$$(L^\dagger)_{i,n+1} = \sum_{j=1}^i (L^{-1})_{i,j} S_{j,n+1}, \quad (25)$$

$$(L^{-1})_{n+1,n+1} = \left(S_{n+1,n+1} - \sum_{i=1}^n (L_{i,n+1}^\dagger)^* L_{i,n+1}^\dagger \right)^{-1/2}, \quad (26)$$

and

$$(L^{-1})_{n+1,i} = - (L^{-1})_{n+1,n+1} \sum_{j=i}^n (L_{j,n+1}^\dagger)^* (L^{-1})_{j,i}. \quad (27)$$

This scheme of transforming Eq. (9) into Eq. (21) is computationally much faster than traditional schemes^{20,22} which involve the diagonalization of the matrix S . It is of particular efficiency for the case of the mixed-basis method. In the present approach, S is a matrix of $(M+N) \times (M+N)$ dimension where N is the number of Bloch sums of localized functions and M is the number of plane waves in the basis set. Since as seen later M is usually 5–10 times larger than N , a large portion of the matrix S is already in the form of Eq. (22) with L^{-1} being the identity matrix for the first M rows and M columns. Hence the recursion relations Eqs. (25)–(27) are only needed to be applied to the remaining part of the matrix to obtain the full L^{-1} matrix. This property of L^{-1} can also be used to simplify the transformations in Eqs. (23) and (24). Once Eq. (9) has been transformed into the standard form, Eq. (21), H' is diagonalized to obtain the energies $E_n(\vec{k})$ and the wave functions $\psi_{n\vec{k}}(\vec{r})$ of the electrons.

For the next step of the self-consistency process, we calculate the total valence-charge density

$$\rho(\vec{r}) = 2 \sum_{n,\vec{k}} \Theta(E_F - E_{n\vec{k}}) |\psi_{n\vec{k}}(\vec{r})|^2, \quad (28)$$

[here $\Theta(x)$ is a step function which is unity for $x > 0$ and zero for $x < 0$]. From $\rho(\vec{r})$, the Hartree screening potential V_H and exchange-correlation potential V_{xc} are calculated via Eqs. (3) and (4). These two screening potentials are then added to the ionic potential to form the new total crystalline potential for the next iteration. The whole

process is repeated until the output screening potentials are self-consistent with respect to the input potentials.²³

We would like to point out here that the fast-Fourier-transform techniques can also be employed to evaluate the Hartree and the exchange-correlation potentials. For example, in solving the Poisson equation in three dimensions to obtain V_H , one either solves the integral equation in real space

$$V_H(\vec{r}) = e^2 \int \frac{\rho(\vec{r}')}{|\vec{r} - \vec{r}'|} d^3r' \quad (29)$$

or transforms Eq. (3) to reciprocal space

$$V_H(\vec{G}) = 4\pi e^2 \rho(\vec{G}) / |\vec{G}|^2. \quad (30)$$

In either case, the number of operations involved is proportional to $(mN)^2$ where m is the number of atoms per unit cell and $N = N_x N_y N_z$ is the size of the mesh for each atom. For transition-metal atoms, N is at least ~ 5000 . Using the fast-Fourier-transform approach, $\rho(\vec{G})$ may be obtained from the wave functions in the order of $(mN) \ln(mN_x) \ln(N_y) \ln(N_z)$ operations. $V_H(\vec{G})$ can then be obtained trivially from Eq. (30). Similarly the exchange-correlation potential $V_{xc}(\vec{G})$ may be evaluated using the same techniques.

III. APPLICATION TO BULK Nb AND Pd

As examples, we have applied the formulation in Sec. II to the calculation of the electronic structure of bulk Nb and Pd. These two metals are of different crystal structure and situated near the beginning and at the end of the $4d$ transition-metal series, respectively. Thus they will provide a good illustration of the accuracy and efficiency of the present method.

A. Gaussian orbitals

For both Nb and Pd, we have used Gaussian orbitals

$$f_m(\vec{r}) = A r^2 e^{-\lambda r^2} Y_{2m}(\theta, \phi) \quad (31)$$

to supplement the plane waves in the basis set. Here

$$A = \left[\frac{16}{15} (2\lambda)^{7/2} (1/\sqrt{\pi}) \Omega_a \right]^{1/2} \quad (32)$$

is a normalization constant and m is an index for the five angular-momentum components of the $l=2$ spherical harmonics. Hence, in addition to the plane waves, the basis set consists of five Bloch sums of the f_m 's for each atom in the unit cell. The Fourier coefficients of the Gaussian orbitals needed in the evaluation of the matrix elements are then given by the following analytic expression

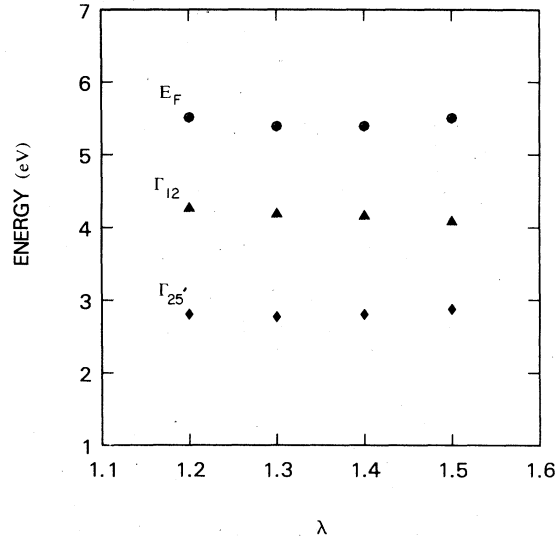


FIG. 1. Band-structure energies of Pd as a function of the Gaussian parameter λ . The \bullet , \blacktriangle , and \blacklozenge indicate the Fermi level and the energies of the lowest Γ_{12} and $\Gamma_{25'}$ states, respectively. These values are calculated self-consistently for each λ with ~ 50 plane waves in the mixed basis.

$$\begin{aligned} f_m(\vec{k}) &= \frac{1}{\Omega_a} \int e^{-i\vec{k}\cdot\vec{r}} f_m(\vec{r}) d^3r \\ &= \frac{4\pi}{\Omega_a} Y_{2m}(\theta_{\vec{k}}, \phi_{\vec{k}}) A \int r^2 dr r^2 e^{-\lambda r^2} j_2(kr) \\ &= \frac{4\pi\sqrt{\pi}}{16\Omega_a} A q^2 \lambda^{-7/2} \exp(-q^2/4\lambda) Y_{2m}(\theta_{\vec{k}}, \phi_{\vec{k}}), \quad (33) \end{aligned}$$

where j_2 is a spherical Bessel function.

The parameter λ is to be determined in such a way so that the set $\{|\phi_{i\mu}\rangle; |\vec{k} + \vec{G}\rangle\}$ will be the most judicious set of functions for the expansion of the crystalline electron wave functions. In traditional tight-binding schemes, one chooses λ by fitting to atomic wave functions. Such procedures are somewhat ambiguous and do not necessarily produce an optimum choice for λ . In the present mixed-basis approach, a λ which optimizes a given basis set is obtained by treating it as a variational parameter in the band-structure calculation. That is, for a given and fixed set of M plane waves, we calculate the band structure and vary λ until we arrive at a λ_{optimum} which minimizes the band-structure energy. However, as seen in Fig. 1 the energy band structure is not very sensitive to the exact value of λ provided sufficient convergence is achieved.

B. Results

The calculated electronic structure for both materials agrees very well with results calculated using other methods and with values deduced from

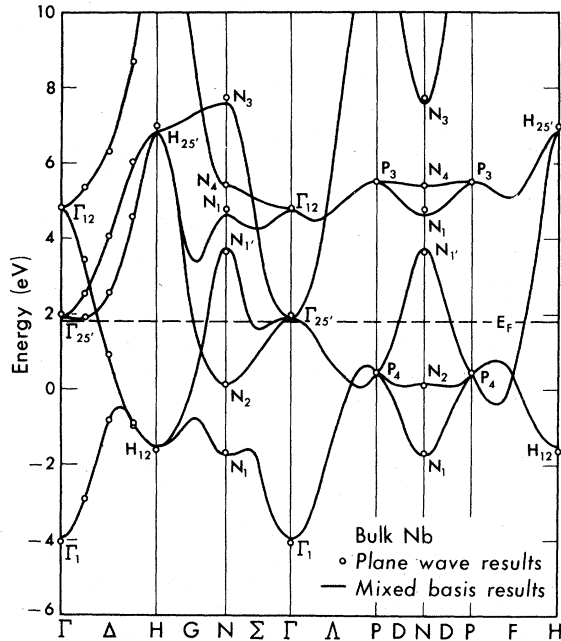


FIG. 2. Self-consistent pseudopotential band structure of Nb. The solid curves are calculated using the mixed-basis method and the circles are values obtained using the plane-wave method.

experiments. Figure 2 depicts the theoretical band structure of Nb. The solid curves are self-consistent energy bands²⁴ calculated using the mixed-basis pseudopotential method and the circles are results obtained using the standard plane-wave approach.²⁵ To obtain highly convergent plane-wave results, ~ 160 plane waves were used in the basis to expand the electron wave function and an additional ~ 100 plane waves were included via the Lowdin perturbation scheme.¹⁹ The mixed-basis results, on the other hand, were obtained using a much smaller basis set consisting of ~ 20 plane waves plus five Bloch sums of the Gaussian orbitals ($\lambda=0.78$ in units of reciprocal Bohr radius squared).

For bulk Nb which contains only one atom per unit cell, the calculations can be carried out with no difficulties using either methods. However, since the numerical effort in both approaches increases as the third power of the number of basis functions used, the saving in computation time is enormous for systems with many atoms per unit cell. For example, in the case of surface calculations with supercells which usually contain ten or more atoms per unit cell, we are dealing with the difference of diagonalizing matrices of the size of a few thousands to that of a few hundreds. A reduction of two to three orders of magnitude in computational effort is achieved with the mixed-basis method.

TABLE I. Comparison of the Nb energy levels at high symmetry points between results calculated using the mixed-basis method and results calculated using the plane-wave method. ($E_F=1.78$ eV.)

| \vec{k} point | Energy (eV) | | |
|-----------------|------------------|-------------|-------|
| | Plane-wave basis | Mixed basis | |
| Γ | Γ_1 | -4.05 | -4.00 |
| | $\Gamma_{25'}$ | 1.94 | 1.89 |
| | Γ_{12} | 4.79 | 4.75 |
| N | N_1 | -1.67 | -1.75 |
| | N_2 | 0.12 | 0.12 |
| | $N_{1'}$ | 3.67 | 3.75 |
| | N_1 | 4.78 | 4.62 |
| P | N_4 | 5.42 | 5.37 |
| | N_3 | 7.74 | 7.59 |
| | P_4 | 0.46 | 0.42 |
| H | P_3 | 5.53 | 5.51 |
| | H_{12} | -1.56 | -1.52 |
| | $H_{25'}$ | 7.00 | 6.82 |

Table I displays the energy eigenvalues of bulk Nb for the various symmetry points in the Brillouin zone. For energies near the Fermi level ($E_F=1.78$ eV), the eigenvalues from the two calculations agree extremely well. The largest discrepancy is 0.18 eV which occurs at $H_{25'}$ at 4.0 eV above the Fermi level. Typically the values from the two calculations are within 0.05 eV of each other. This agreement is quite remarkable considering the small number of basis functions used in the mixed-basis approach and the very different approximations used in the two methods. The calculated band structure is also in good agreement with experiments and with results calculated using other methods.²⁵ A detailed comparison of the pseudopotential results to other results has been presented in Ref. 25.

Another critical test for the mixed-basis method is the accuracy of the calculated electron wave functions. Figure 3 shows the calculated valence-charge density as a function of distance between nearest-neighboring Nb atoms. Since these are pseudopotential results, the charge density is smooth in the core region and is at a minimum at the atomic site. As seen from Fig. 3, the two calculated charge-density distributions are essentially the same with the density from the mixed-basis calculation slightly more localized near the atom cores. This small difference results from the fact that, for a basis set of finite size, the plane waves tend to emphasize the delocalized character of the wave function whereas the Gaussian orbitals tend to emphasize the atomiclike character of the wave function near the core. With an increase in the size of the basis set in both approaches, the charge density will converge to a density distribution

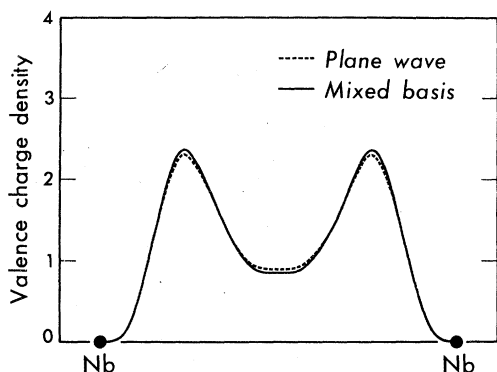


FIG. 3. Total valence-charge density along the direction between nearest-neighbor Nb atoms. The solid curve is the self-consistent pseudo charge density calculated in the mixed-basis approach. The dash curve is calculated using a plane-wave basis. The charge density is normalized to one electron per unit cell.

intermediate between the values shown in Fig. 3.

Similarly, by going from the plane-wave basis to the mixed basis, a large reduction in the number of basis functions can be achieved for the case of bulk Pd. Because the d electrons are much more tightly bound to the atomic core for Pd than Nb, in the plane-wave approach, approximately 400–500 plane waves are needed to obtain convergent wave functions. Comparable results may be obtained in the mixed-basis approach by using a basis set consisting of ~ 40 plane waves plus five Bloch sums of Gaussian orbitals ($\lambda=1.37$). The calculated results for the \vec{k} points Γ and L are shown in Table II together with experimental values deduced from angular-resolved photoemission measurements²⁶ and with theoretical results from previous calculations.^{27–30} As seen from Table II, the agreement appears to be excellent.

IV. SUMMARY AND DISCUSSIONS

In summary, we have formulated a mixed-basis method for the calculation of the electronic structure of solids. Results for the band structure of bulk Pd and Nb are presented. It is shown that the present method combines the advantages of many traditional methods and avoids many of their disadvantages. As in the plane-wave pseudopotential method,²³ the calculations are carried out in a self-consistent-field fashion with no restrictions on the shape of the crystalline potential. The number of basis functions, on the other hand, has been greatly reduced by the presence of the localized functions in the basis set. Because of these features, the present method is ideally suited for calculating the electronic properties of systems with complicated, open structure which contain both highly localized and delocalized electrons.

In the cases of Nb and Pd, upon the inclusion of d -like Gaussian orbitals in the basis set, the number of plane waves needed is found to be reduced by an order of magnitude. The physical basis for this reduction is the following. The higher-component (i.e., the short wavelength) \vec{G} vectors are required mainly to reproduce the short-range, atomiclike character of the electrons near the atomic cores. In the mixed-basis approach, this role is taken over by the localized orbitals. The function of the plane waves is to complement the localized functions in forming the crystalline wave function in all space. Since, even for the pure d states in the band structure, the localized orbitals are not exact solutions of the crystalline potential, the limiting factor on the number of plane waves in the basis set is then the number of intermediate wavelength \vec{G} vectors required to supplement the

TABLE II. Comparison of energy levels at Γ and L between the present calculation of the Pd band structure and previous theoretical results. Also indicated are the latest experimental results from angular-resolved photoemission measurements.

| \vec{k} point | Band number | Experiment ^a | Present work | Moruzzi <i>et al.</i> ^b SCKKR | Muller <i>et al.</i> ^c 4d ¹⁰ HFS | Andersen ^d Christensen ^e RAPW |
|-----------------|-------------|----------------------------------|--------------|---|---|---|
| Γ | 2, 3, 4 | -2.55 ± 0.15 | -2.56 | -2.68 | -2.59 | -2.79 -2.49 |
| Γ | 5, 6 | -1.15 ± 0.1 | -1.21 | -1.23 | -1.19 | -1.17 -2.98 |
| L | 2, 3 | -2.4 ± 0.2 | -2.66 | -2.78 | -2.70 | -2.62 -0.14 |
| L | 4, 5 | -0.4 ± 0.2 -0.1 ± 0.1 | -0.09 | -0.05 | -0.06 | +0.05 |

^aReference 26.

^bReference 27. SCKKR: self-consistent KKR.

^cReference 28. HFS: Hartree-Fock-Slater.

^dReference 29.

^eReference 30. RAPW: relativistic APW.

localized orbitals in providing a convergent expansion of the crystalline wave functions.

From our experience with Nb and Pd, we find that, in addition to the five local orbitals, approximately 20–40 plane waves per atom are required to form a convergent basis set for transition metal atoms. This number is comparable to the size of the basis set in traditional APW and KKR calculations. However, as mentioned earlier, the muffin-tin approximation to the crystalline potential is removed in the present method. This aspect of the method enables one to obtain reliable results for a number of interesting systems with open structure.³¹ Recently, the present approach has been applied successfully to study the electronic structure and photoemission properties of clean^{14,32} and chemisorbed³³ transition-metal surfaces and to examine some of the unusual properties of the A-15 compounds.¹⁵

Finally we would like to remark that the present formulation is not necessarily restricted to using pseudopotentials. It can be extended straightforwardly to perform rigid-core, *ab initio* calculations. In this case, the core states must be incorporated into the basis set either as additional basis functions or through orthogonalization procedures.

ACKNOWLEDGMENTS

One of the authors (S.G.L.) would like to thank A. R. Williams for helpful discussions. Research was supported in part by NSF Grant No. DMR76-20647-A01 and by the Division of Basic Energy Sciences, U. S. Department of Energy.

APPENDIX A

Equations (25)–(27) can be easily derived from the definition of the matrix L . L is defined to be in the lower triangular form, i.e., $L_{ij}=0$ if $j>i$.

Let us define $S(n)$ to be a $n \times n$ matrix which is composed of the first n rows and first n columns of the overlap matrix S and define $L(n)$ to be the Choleski decomposition of $S(n)$, i.e.,

$$S(n) = L(n)[L(n)]^\dagger. \quad (\text{A1})$$

We would like to find the Choleski decomposition for $S(n+1)$ assuming that we know $L(n)$.

Since $L(n+1)$ is lower triangular, we have

$$\begin{aligned} L(n+1)[L(n+1)]^\dagger &= \begin{pmatrix} L(n) & 0 \\ b^\dagger & x \end{pmatrix} \begin{pmatrix} L(n)^\dagger & b \\ 0 & x \end{pmatrix} \\ &= \begin{pmatrix} S(n) & a \\ a^\dagger & y \end{pmatrix} \end{aligned} \quad (\text{A2})$$

where $a^\dagger = (S_{n+1,1}, \dots, S_{n+1,n})$, $y = S_{n+1,n+1}$, $b^\dagger = (L_{n+1,1}, \dots, L_{n+1,n})$, and $x = L_{n+1,n+1}$. We therefore immediately arrive at

$$b = [L(n)]^{-1}a, \quad (\text{A3})$$

which is just Eq. (25), i.e.,

$$(L^\dagger)_{i,n+1} = \sum_{j=1}^i (L^{-1})_{i,j} S_{j,n+1}. \quad (\text{A4})$$

Next we write the identity matrix in the form

$$\begin{pmatrix} I(n) & 0 \\ 0 & 1 \end{pmatrix} = \begin{pmatrix} L(n) & 0 \\ b^\dagger & x \end{pmatrix} \begin{pmatrix} L^{-1}(n) & 0 \\ c^\dagger & z \end{pmatrix}, \quad (\text{A5})$$

where $c^\dagger = (L_{n+1,1}^{-1}, \dots, L_{n+1,n}^{-1})$ and $z = (L^{-1})_{n+1,n+1}$. z is then equal to x^{-1} which is $(y - b^\dagger b)^{-1/2}$. Hence

$$(L^{-1})_{n+1,n+1} = \left(S_{n+1,n+1} - \sum_{i=1}^n (L_{i,n+1}^\dagger)^* L_{i,n+1}^\dagger \right)^{-1/2}. \quad (\text{A6})$$

Finally from

$$b^\dagger L^{-1}(n) + xc^\dagger = 0 \quad (\text{A7})$$

we have

$$c^\dagger = -b^\dagger L^{-1}(n)/x \quad (\text{A8})$$

and therefore

$$(L^{-1})_{n+1,i} = - (L^{-1})_{n+1,n+1} \sum_{j=i}^n (L_{j,n+1}^\dagger)^* (L^{-1})_{j,i}. \quad (\text{A9})$$

*Present address.

¹*Interactions on Metal Surfaces*, edited by R. Gomer (Springer-Verlag, Berlin, 1975); *Surface Physics of Materials*, edited by J. M. Blakely (Academic, New York, 1975), Vols. 1 and 2.

²L. R. Testardi, in *Physical Acoustics*, edited by W. P. Mason and R. N. Thurston (Academic, New York, 1973), Chap. 10, p. 193; M. Weger and I. B. Goldberg, in *Solid State Physics*, edited by F. Seitz and D. Turnbull (Academic, New York, 1973), Vol. 28, p. 1.

³U. Köster, K. N. Tu, and P. S. Ho, *Appl. Phys. Lett.*

31, 634 (1977), and references therein.

⁴P. C. Hohenberg and W. Kohn, *Phys. Rev.* **136**, 864 (1964); W. Kohn and L. Sham, *Phys. Rev.* **140**, 1133 (1965).

⁵K. S. Singwi, A. Sjolander, P. M. Tosi, and R. H. Land, *Phys. Rev. B* **1**, 1044 (1970).

⁶For example, in a recent self-consistent tight-binding calculation of a three-layer Cu thin film [J. A. Appelbaum and D. R. Hamann, *Bull. Am. Phys. Soc.* **23**, 364 (1978) and unpublished], a large basis consists of Gaussians of various sizes located at 47 different

sites are required for the expansion of the potential and the electron charge density. Also supplementary floating Gaussian wave functions of s and p character outside the surface atoms are found to be needed to allow for additional variational freedom in the vacuum region. The sizes and sites of the Gaussians are determined from experimentation and, at each stage of the self-consistency cycle, the charge density and the potential have to be refitted using the Gaussians.

⁷L. Hodges, H. Ehrenreich, and N. D. Lang, Phys. Rev. **152**, 505 (1966).

⁸R. A. Deegan and W. D. Twose, Phys. Rev. **164**, 993 (1967).

⁹F. A. Butler, F. K. Bloom, Jr., and E. Brown, Phys. Rev. **180**, 744 (1969), and references therein.

¹⁰A. B. Kunz, Phys. Rev. **180**, 934 (1969).

¹¹R. N. Euwema, Phys. Rev. B **4**, 4332 (1971).

¹²C. Friedli and N. W. Ashcroft, Phys. Rev. B **16**, 662 (1977).

¹³Approximately 20 to 40 basis functions per atom are found to be needed for bulk transition metals. This number is comparable to the size of the basis set in APW and KKR calculations but in an order of magnitude smaller than the number of basis functions needed in a totally plane-wave approach. Since the present method has the flexibility and the accuracy of the plane-wave approach, it is therefore more desirable than the tradition APW and KKR methods for studying systems such as those mentioned in the Introduction.

¹⁴S. G. Louie, Phys. Rev. Lett. **40**, 1525 (1978).

¹⁵P. B. Allen, W. E. Pickett, K. M. Ho, and Marvin L. Cohen, Phys. Rev. Lett. **40**, 1532 (1978); K. M. Ho, W. E. Pickett, and Marvin L. Cohen, Phys. Rev. Lett. **41**, 580 (1978).

¹⁶For example, the functional form given by L. Hedin and B. I. Lundqvist, J. Phys. C **4**, 2064 (1971).

¹⁷J. C. Slater, *Self-consistent Field for Molecules and Solids* (McGraw-Hill, New York, 1974).

¹⁸The validity of using the pseudo charge densities in self-consistent calculations can be seen as follows. In the local-density theory of exchange and correlation (Refs. 4, 5, and 17), the exchange-correlation potential is a functional of $\rho_{\text{total}} = \rho_v + \rho_c$ where ρ_v is the valence-charge density and ρ_c is the core-charge density. The exchange-correlation potential can be rewritten as $V_{xc}(\rho_{\text{total}}(\vec{r})) = [V_{xc}(\rho_v(\vec{r}) + \rho_c(\vec{r})) - V_{xc}(\rho_{\text{pv}}(\vec{r}))] + V_{xc}(\rho_{\text{pv}}(\vec{r}))$, where ρ_{pv} is the pseudo-valence-charge density. At distances outside of the ion core, $\rho_{\text{pv}} = \rho_v$ and $\rho_c = 0$. Hence $V_{xc}(\rho_{\text{total}}(\vec{r}))$

$= V_{xc}(\rho_{\text{pv}}(\vec{r}))$. In the core region, ρ_{pv} will be quite insensitive to the environment of the atom. We may include the above bracketed term into the ionic pseudopotential. Therefore $V_{xc}(\rho_{\text{total}})$ again is replaced by $V_{xc}(\rho_{\text{pv}})$. Similar arguments hold for the Hartree potential.

¹⁹M. L. Cohen and V. Heine, in *Solid State Physics*, edited by H. Ehrenreich, F. Seitz, D. Turnbull (Academic, New York, 1970), Vol. 24, p. 37.

²⁰D. J. Chadi, Phys. Rev. B **16**, 790 (1977).

²¹F. E. Harris and H. J. Monkhorst, Phys. Rev. Lett. **23**, 1026 (1969); A. Mauger and M. Lannoo, Phys. Rev. B **15**, 2324 (1977); J. L. Fry, N. E. Brener, and R. K. Bruyere, Phys. Rev. B **16**, 5225 (1977); N. E. Brener and J. L. Fry, Phys. Rev. B **17**, 506 (1978).

²²B. Wendroff, *Theoretical Numerical Analysis* (Academic, New York, 1966); J. Wilkinson, *Algebraic Eigenvalue Problem* (Oxford University Press, Oxford, 1966).

²³For a detailed discussion of the self-consistent iterating process, see, for example, S. G. Louie and M. L. Cohen, Phys. Rev. B **13**, 2461 (1976).

²⁴To facilitate comparison with previous calculations (Ref. 25), the exchange-correlation parameter α has been set to 0.8 for the Nb calculation. For the Pd calculation, we used the functional form given in Ref. 16 for α .

²⁵K. M. Ho, S. G. Louie, J. R. Chelikowsky, and M. L. Cohen, Phys. Rev. B **15**, 1755 (1977), and references therein.

²⁶F. J. Himpsel and D. E. Eastman, Phys. Rev. B **18**, 5236 (1978).

²⁷V. L. Moruzzi, J. F. Janak, and A. R. Williams, *Calculated Electronic Properties of Metals* (Pergamon, New York, 1978).

²⁸F. M. Mueller, A. J. Freeman, J. O. Dimmock, and A. M. Furdyna, Phys. Rev. B **1**, 4617 (1970).

²⁹O. K. Andersen, Phys. Rev. B **2**, 883 (1970).

³⁰N. E. Christensen, Phys. Rev. B **14**, 3446 (1976).

³¹Recent developments in the linearized-augmented-plane-wave (LAPW) method have also permitted realistic calculations for thin films. See, for example, O. Jepsen, J. Madsen, and O. K. Andersen, Phys. Rev. (to be published); H. Krakauer, M. Posternak, and A. J. Freeman, *ibid.* (to be published); and D. R. Hamann (private communications).

³²G. P. Kerker, K. M. Ho, and M. L. Cohen, Phys. Rev. Lett. **40**, 1593 (1978).

³³S. G. Louie, Phys. Rev. Lett. (to be published).